High-Speed MAS ^{19}F NMR Analysis of an Irradiated Fluoropolymer

T. R. Dargaville,[†] G. A. George,[‡] D. J. T. Hill,*[,†] U. Scheler,[§] and A. K. Whittaker[†]

Polymer Materials and Radiation Group, University of Queensland, St Lucia, QLD 4072, Australia; Queensland University of Technology, Brisbane, QLD 4001, Australia; and Institute of Polymer Research Dresden, Hohe Strasse 6 01069 Dresden, Germany

Received February 6, 2002

ABSTRACT: The effect of γ-radiation on a perfluoroalkoxy (PFA) resin was examined using solid-state high-speed magic angle spinning (MAS) ^{19}F NMR spectroscopy. Samples were prepared for analysis by subjecting them to γ-radiation in the dose range 0.5−3 MGy at either 303, 473, or 573 K. New structures identified include new saturated chain ends, short and long branches, and unsaturated groups. The formation of branched structures was found to increase with increasing irradiation temperature; however, at all temperatures the radiation chemical yield (*G* value) of new chain ends was greater than the *G* value of long branch points, suggesting that chain scission is the net process.

1. Introduction

Perfluoroalkoxy (PFA) resin is a copolymer of tetrafluoroethylene (TFE) and a perfluoroalkyl vinyl ether. PFA exhibits many of the desirable properties of the homopolymer, poly(tetrafluoroethylene) (PTFE), such as excellent thermal stability, low surface energy, and chemical inertness. The advantage of PFA over PTFE is its lower melt viscosity which facilitates fabrication using standard melt processing techniques; PTFE is limited to molding using elaborate manufacturing methods.

Because of the insolubility of many fluoropolymers, any characterization is restricted to solid-state techniques. While the characterization of irradiated PTFE has been widely studied,[1−4] the radiolytic behavior of PFA has received less attention in the literature. Chain scission has been identified as the main radiolytic process when PFA is irradiated at room temperature, based on a decrease in the melting point[5] and a decrease in the tensile strength and elongation with increasing dose, as measured by tensile testing.[6−8] FTIR spectroscopy of irradiated PFA films has been used to identify carboxylic acid end groups and unsaturated groups.[9]

Recently, solid-state high-speed MAS ^{19}F NMR has been used to characterize PTFE irradiated at room temperature,[10] PTFE irradiated in the melt,[10,11] and FEP (copolymer of tetrafluoroethylene and hexafluoropropylene) irradiated below and above the glass transition temperature.[12] In this study we have used the same NMR technique to investigate the new structures formed in the nonvolatile component of PFA after exposure to γ-radiation over the temperature range 303−573 K in a vacuum as well as in air at 303 K.

2. Experimental Section

PFA (DuPont, pellets) samples were exposed to γ-radiation at either the Australian Nuclear Science and Technology Organisation (ANSTO) or the University of Queensland. Irradiation at 303 K was performed using a dose rate of 5.9 kGy/h, while irradiation at higher temperature was performed using a dose rate of 1.5 kGy/h. Samples to be irradiated in a vacuum were evacuated at 10^{-4} Torr in glass tubes for 24 h before being sealed. All samples with the exception of the samples irradiated in the presence of air were heated at 473 K after irradiation for 2 h to remove the majority of the radicals before being opened to the atmosphere. Samples irradiated in the presence of air were not thermally treated after irradiation. All samples were cryogenically milled into powders for NMR analysis.

Single-pulse NMR experiments were performed using a Bruker 300 MHz NMR spectrometer with a H/F-X BL 2.5 probe with the high-frequency channel tuned to a ^{19}F resonance frequency of 282 MHz. Samples were spun at a frequency of 32 kHz at the magic angle using a 2.5 mm o.d. rotor. The recycle time used (10 s) was long enough to obtain quantitative integrated peak intensities. Spectra were acquired using a $\pi/2$ pulse duration of 3 μs. ^{19}F chemical shifts are reported relative to the CF_2 signal of PTFE at −122 ppm, which was externally referenced to $CFCl_3$. The broad signal due to static fluorine in probe materials was removed using a spline baseline correction algorithm.

Hahn echo experiments were performed using a MSL 300 spectrometer operating at 282 MHz with a Doty Scientific triple-resonance MAS probe. Samples were spun at a frequency of 20.5 kHz at the magic angle using a 4 mm o.d. rotor. Spectra were acquired using a $\pi/2$ pulse duration of 6 μs and a total echo time of 10 ms. The method of referencing and removal of the static fluorine signal was the same as for the single-pulse experiments.

FTIR spectra were recorded on a Bio-Rad FTS-155 spectrometer. Samples were prepared by pressing PFA pellets under 4 tonnes of pressure at room temperature. Intensities in the spectra were normalized to the CF_2 backbone overtone at 2365 cm^{-1}.

3. Results and Discussion

3.1. Untreated PFA. Assignment of the peaks in the ^{19}F NMR spectrum of untreated PFA (Figure 1a) are shown in Table 1. These assignments were made according to tables of chemical shifts[13a,b] and on the expected peak area ratios. The perfluoroalkoxy comonomer was identified as perfluoropropyl vinyl ether (PPVE). The fraction of this comonomer was determined from the relative peak area of the PPVE groups to TFE groups. The mole percent of the comonomer in untreated PFA was 1.7 ± 0.2%.

The peak due to perfluoromethyl chain ends would be expected to appear at approximately −83 to −84 ppm,[13c] which would overlap with the peak due to the

[†] University of Queensland.
[‡] Queensland University of Technology.
[§] Institute of Polymer Research Dresden.
* To whom correspondence should be addressed.

10.1021/ma020195q CCC: $22.00
Published on Web 06/04/2002

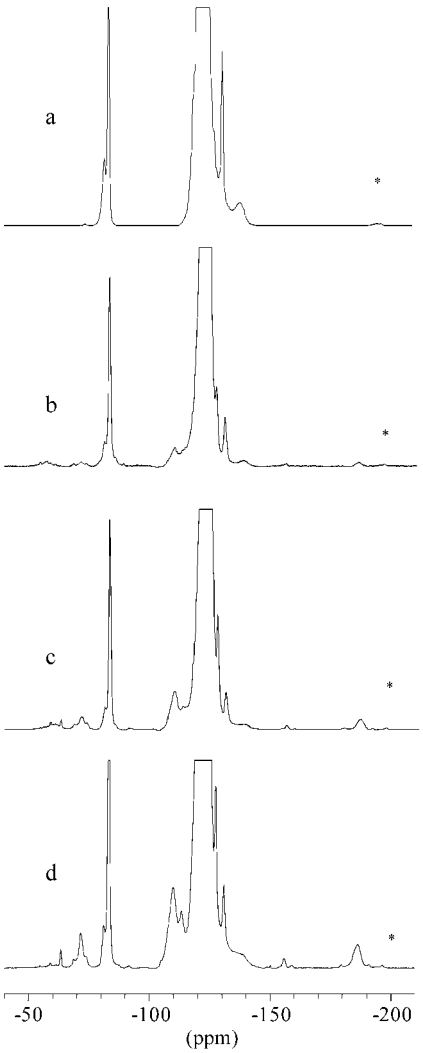

Figure 1. ^{19}F MAS NMR of PFA: (a) untreated PFA, (b) irradiated to 1 MGy at 303 K, (c) irradiated to 1 MGy at 473 K, (d) irradiated to 1 MGy at 573 K. Spinning sidebands from the CF_3 groups are denoted by an asterisk.

Table 1. Assignments of Peaks in ^{19}F NMR Spectra of Untreated PFA

Structure	Chemical shift (ppm)
—CF_2–C**F**$_2$–CF_2—	-110 to –129 (centre at –122)
~~CF_2–CF(O–C**F**$_2$–CF_2–CF_3)–CF_2~~	-81.8
~~CF_2–CF(O–CF_2–C**F**$_2$–CF_3)–CF_2~~	-130.9
~~CF_2–C**F**(O–CF_2–CF_2–CF_3)–CF_2~~	-138.5
~~CF_2–C**F**$_3$	-83.6

CF_3 of the PPVE side chains, making them indistinguishable. We compared the area of the peak at −83.6 ppm with that due to the OC**F**$_2$ peak, taking into account the different number of fluorine nuclei, to determine whether a portion of this peak was due to perfluoromethyl chain ends. We found that there was no excess peak area under the peak at −83.6 ppm; therefore, the molecular weight of the untreated material must exceed the uncertainty in the measurement of the CF_3 peak area. We estimate this to be ±5%; therefore, the minimum molecular weight of the untreated PFA would be at least 1.2×10^5 g/mol.

3.2. Irradiated PFA. 3.2.1. Radiolytic Products from TFE Groups. Because of the low probability of addition of PPVE monomer units during synthesis of PFA, we would expect that the PPVE units would be isolated in the copolymer.[14] Indeed, the NMR spectrum of the untreated material suggests this is the case with no evidence of sequence effects. Given that the PFA used was composed of 98.3 ± 0.2 mol % tetrafluoroethylene (TFE) units, the majority of the radiolytic products would be expected to be the same as for PTFE, although the different morphology, glass transition, and crystalline melting temperatures of PFA may be expected to affect the temperature at which various products are formed. Fuchs and Scheler[10] and Katoh et al.[11] have both reported the high-speed ^{19}F MAS NMR of irradiated PTFE. Katoh et al. used spinning speeds of 12 and 15 kHz, and while at these speeds the spinning sidebands overlap with peaks of interest, by using two spinning speeds they were able to shift the spinning sidebands so that between the two spectra recorded at different speeds most of the isotropic peaks could be observed. Fuchs and Scheler used higher spinning speeds of 35 kHz to remove the spinning sidebands from the region of interest altogether.

When PTFE was irradiated at room temperature, Fuchs and Scheler observed just two new peaks at approximately −82 and −126 ppm attributed to new C**F**$_2$C**F**$_3$ chain ends. For PTFE irradiated in the melt, Fuchs and Scheler[10] and Katoh et al.[11] observed a number of new structures which were consistent with branching, including CF_3 side groups and Y branching points. Chain-end structures include CF_3 groups on saturated chain ends, COF end groups, and CF_3 groups adjacent to double bonds. Fuchs and Scheler concluded that PTFE cross-links when irradiated in the melt based on the excess of branch points over chain ends. Katoh et al. measured the cross-linking density and G value of cross-linking based only on the intensity of the tertiary CF peak, which does not distinguish between cross-links and long-chain branches.

Figure 1b−d shows the ^{19}F NMR spectra of the nonvolatile products of PFA irradiated with γ-radiation to 1 MGy at 303, 473, and 573 K all in a vacuum. The peak assignments are shown in Table 2 as well as a comparison with the assignments made by Katoh et al. and Fuchs and Scheler for PTFE irradiated in the melt. The major products formed from radiolysis are the same as in PTFE irradiated in the melt, although in different proportions depending on the radiation temperature. Spectra of samples irradiated to other doses (not shown) indicate the same structures, only in different proportions for each respective temperature.

The spectra in Figure 1b−d show two peaks at −71.7 and −68.6 ppm. These are assigned to CF_3 side chains in different morphological environments based on their different T_2 relaxation times implied from the Hahn echo experiment shown in Figure 2. In the Hahn echo experiment the peaks decrease in intensity compared with the single-pulse experiment due to the spin−spin or T_2 relaxation times of the nuclei. More mobile groups,

Table 2. Assignments of Peaks in ^{19}F NMR Spectra of PTFE Irradiated in the Melt by Katoh et al.[11] and Fuchs and Scheler[10] and Our Assignments for New Peaks in Irradiated PFA

Structure	Katoh *et al.* PTFE irradiated in melt	Fuchs and Scheler PTFE irradiated in melt	Our assignments PFA irradiated at 303, 473, 573 K
~~CF_2–CF_3	-84	-82	-83.6
~~CF_2–CF_3	-128	-126	-127.6
–CF–	-190	-185	-186.4
R_f–CF_2–R_f	-124, -110, -120	-122	-122
–CF_2–CF(–CF_2–)–CF_2–	not specifically assigned	-108	-109.8
–CF_2–CF(CF_3)–CF_2–	not specifically assigned	-111	-113.3
–CF_2–CF(CF_3)–CF_2–	-72	-72	-68.6 (crystalline) -71.7 (amorphous)
>CF–CF<	not resolved	-154	-
$R_f$$R_f$>C=C<$CF_3$$R_f$	-59, -60, -62	not assigned	not assigned
CF_2=CF–CF_2–	not observed	not observed	-91.6, 108.6
CF_2=CF–CF_2–	"	"	-190.9
CF_3–CF=CF– or $(CF_3)_2$–CF–	"	"	-73.5
R_f–CF=CF–R_f	"	"	-150.3, -155.7, -158.9

for example chain ends, have longer T_2 times, and their respective peaks will decrease in intensity less than peaks attributed to less mobile (shorter T_2 relaxation times) species in the Hahn echo experiment. The peaks over the range −108 to 128 ppm associated with the in-chain methylene C**F**$_2$ groups are significantly attenuated relative to the more mobile fluoromethyl peaks. The peak at −68.6 ppm has a shorter T_2 relaxation time than the peak at −71.9 ppm, suggesting the CF_3 side chain due to the former is less mobile and perhaps incorporated into the crystalline lattices, whereas the latter are due to CF_3 side chains in the more mobile amorphous regions. It has been shown by several authors that CF_3 groups can be incorporated into the crystalline lattice as point defects in FEP.[15−17] The same two peaks have been observed in untreated FEP and the different $T_{1\rho}$ times measured.[18] It is known that the crystallinity of PTFE irradiated in the melt decreases with increasing dose[19] and changes from opaque to transparent,[20] indicating decreasing degree of crystallinity. Although unassigned by Fuchs and Scheler, their spectra of PTFE irradiated in the melt includes a peak at −68 ppm, which decreases in intensity compared to the peak at −72 ppm with increasing dose and cross-linking, supporting our assignment of the peak at −68.6 ppm being due to CF_3 side chains within the crystal lattices. The same peak was not resolved by Katoh et al. due to incomplete averaging of dipole−dipole coupling at the lower spinning speeds they used. Adjacent to the two CF_3 side chain peaks in our spectra is a peak at −73.5 ppm with very long T_2, suggesting it is on the end of a chain, and we propose that it is due to either C**F**$_3$ groups adjacent to a double bond[13c] or CF(C**F**$_3$)$_2$ groups.[13d]

The formation of unsaturated groups in PFA samples irradiated at 473 and 573 K has been confirmed using FTIR (Figure 3). The band at 1785 cm^{-1} is attributed to terminal double bonds while bands at 1730 and 1717 cm^{-1} are attributed to internal double bonds.[9,21] Previously, Fisher and Correlli[22] postulated that similar bands between 1735 and 1715 cm^{-1} observed in the IR spectra of irradiated PTFE were due to branching points; however, we tend to favor the assignment by Lappan et al.[21] and Lunkwitz et al.[9] of these bands as being due to internal double bonds and support this with

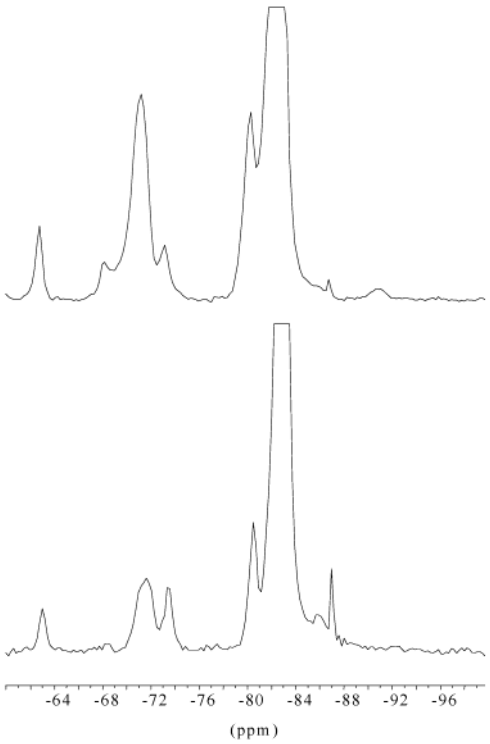

Figure 2. Hahn echo experiment: single-pulse experiment (top); Hahn echo experiment (bottom). The spectra have been normalized to the fluoromethyl peak at −83.6 ppm.

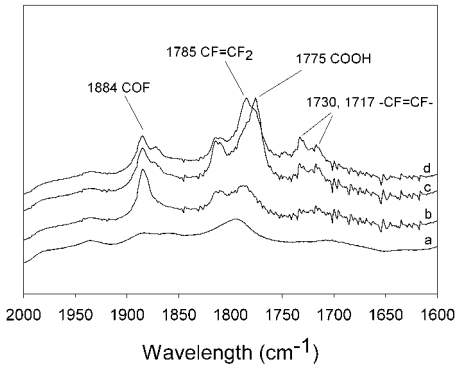

Figure 3. FTIR of PFA: (a) untreated, (b) irradiated to 0.5 MGy at 303 K, (c) irradiated to 0.5 MGy at 473 K, (d) irradiated to 0.5 MGy at 573 K. Assignments were made according to Lappan et al.[21] and Lunkwitz et al.[9]

NMR evidence. In addition, we also found that the samples irradiated at 573 K changed from translucent to black, suggesting some conjugation of double bonds. Similar observations were made by Tutiya[23] for PFA irradiated under analogous conditions to those used here. To prove that the color change was due to radiation *and* heat, we heated a control sample at 573 K for a time corresponding to the radiation time and found that it did not discolor or reveal any new peaks by NMR.

In the ^{19}F MAS NMR spectra of PTFE irradiated in the melt, Fuchs and Scheler assign the peak at −154 ppm to ⟩C**F**−C**F**⟨, while this peak is not resolved in the spectra of Katoh et al. This type of structure seems doubtful due to the unlikelihood of combination of alkyl radicals,[24,25] and we have assigned this peak as well as peaks at −150.3 and −158.9 ppm to either C**F**═C**F**−CF_3 or C**F**═C**F**− groups on the basis of tabulated chemical shifts.[13c] Observation of the terminal unsaturated group peaks is less ambiguous; the peaks at −91.6 and −108.6 ppm are assigned to the fluoromethylene group, and the peak at −190.9 ppm is assigned to the fluoromethine group of the unsaturated group C**F**═C$\mathbf{F_2}$.[13a]

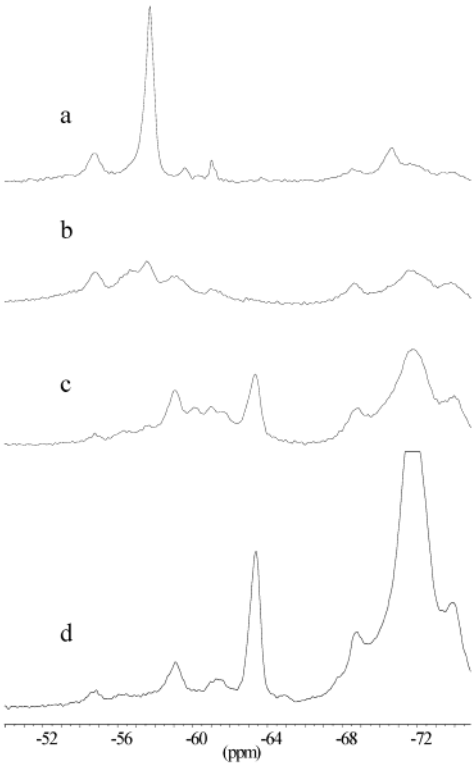

Figure 4. ^{19}F MAS NMR of PFA: expansion of the area from −50 to −75 ppm: (a) PFA irradiated to 1 MGy at 303 K in air, (b) PFA irradiated to 1 MGy at 303 K in a vacuum, (c) irradiated to 1 MGy at 473 K in a vacuum, (d) irradiated to 1 MGy at 573 K in a vacuum.

A number of relatively small peaks in the region −54 to −64 ppm appear in the NMR of PFA samples irradiated across the temperature range studied. An expansion of this region is shown in Figure 4. The most prominent peak in the spectrum of PFA irradiated in air (Figure 4a) in this region is the peak at −57.8 ppm. This is assigned to an oxygenated species, $-OCF_3$ on a chain end,[26] which we also see when PFA is irradiated at 303 K under vacuum (Figure 4b). As the irradiation temperature is increased, the proportions of these peaks change and new peaks at −59.1, −61.4, and −63.4 ppm become significant. Peaks in this region have also been observed in the spectra of Katoh et al. and Fuchs and Scheler for PTFE irradiated in the melt and in FEP irradiated at 300 and 363 K.[12] Attempts to assign these peaks have not been made except by Katoh et al., who postulate that the peaks at −59, −60, and −62 ppm are due to a CF_3 group adjacent to a double bond at a branch point. However, in earlier work with fluoro-oligomers they assigned peaks with similar chemical shifts to C**F**═C$\mathbf{F_2}$ and C(C$\mathbf{F_3}$)$_3$.[27] We cannot unequivocally assign these peaks at this stage.

The peak at −186.4 ppm has been assigned to C**F** branch points. These will be associated with fluoromethyl and longer branches. In our previous work[28] we identified both the main chain ($-CF_2-C^{\bullet}F-CF_2-$) and end-chain radicals ($-CF_2-C^{\bullet}F_2$) in irradiated PFA. Formation of long branches may occur when these two radicals recombine. For the short CF_3 side chains to form we postulate that $^{\bullet}CF_3$ radicals directly combine with the main-chain radical.

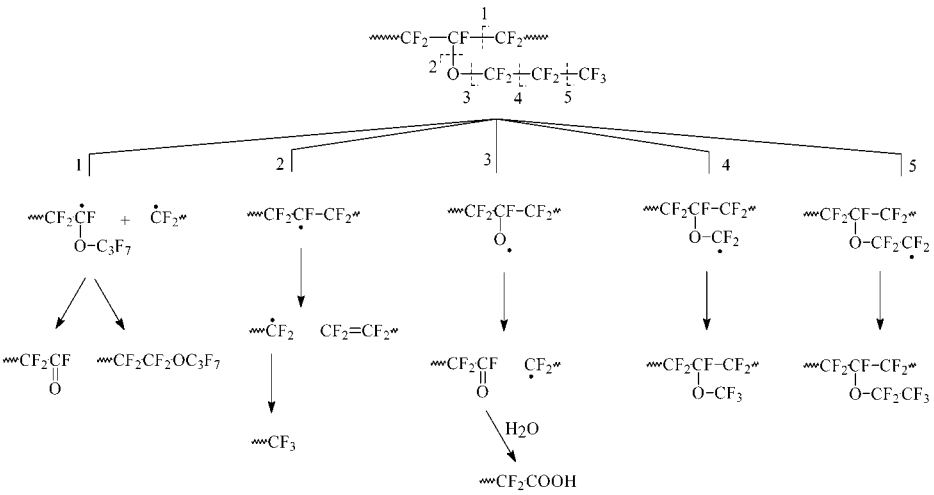

Figure 5. Possible pathways for the reaction of the PPVE units during radiation treatment of PFA.

3.2.2. Radiolytic Products from PPVE Groups. The products formed from the perfluoropropyl vinyl ether (PPVE) groups in PFA are not as evident as the products from extended sequences of TFE units due to the low amount of PPVE present in the untreated material. The relative peak area of peaks at −138.5, −81.8, and −130.9 ppm decrease with increasing dose at all the temperatures studied, implying that PPVE is being consumed. Figure 5 shows all the possible products from bond scission at the PPVE units. Peaks due to acyl fluoride groups (pathways 1 and 3) were observed at +23 ppm (not shown) in samples irradiated at 303 K and decreased in intensity with increasing irradiation temperature. Further reaction of the acyl fluoride with atmospheric moisture would form a carboxylic acid group. Because of overlapping signals, no peak due to the C**F**$_2$COOH group was resolved in the NMR (expected −118 ppm[29]), although we did observe COOH (1775 cm^{-1}) in the FTIR as well as COF (1884 cm^{-1}) (Figure 3).

Pathways 4 and 5 in Figure 5 would yield methyl ether and ethyl ether side chains, respectively. The expected chemical shift for the OC**F**$_3$ of the methyl ether is −52.4 ppm,[30] while for the ethyl ether peaks at −87.6 and −86.0 ppm[13b,e] would be predicted for the OCF$_2$C**F**$_3$ and OC**F**$_2$CF$_3$ groups, respectively. It is difficult to identify peaks at these chemical shifts above the noise in the single-pulse experiments. In the Hahn echo experiment (Figure 2) we observed enhancement of peaks at −87.6 and −86.0 ppm, allowing us to identify the ethyl ether in small amounts. The enhancement of the ethyl ether peaks in the Hahn echo experiment is indicative of its location in the amorphous regions, as would be expected. Curiously, no OC**F**$_3$ side chain of the methyl ether was seen at −52.4 ppm, suggesting either pathway 4 is not important or that the methyl ether is not the end product.

3.3. *G* Values. The radiation chemical yields for the formation of the new chemical structures are expressed as *G* values, which are the number of new structures formed on the deposition of 16 × 10^{-18} J (16 aJ or 100 eV) of energy. The *G* values were calculated from plots of the number of new functional groups against dose for PPVE units, short CF$_3$ side chains, long branches, and CF$_3$ chain ends. *G* values were derived from the initial slopes of these plots, as shown in Figure 6. Because of overlap of the CF$_3$ of the PPVE side chains and new CF$_3$ chain ends, the proportion of the peak at −83.6 ppm due to new CF$_3$ end groups was taken as the excess after subtracting the area due to CF$_3$ of the PPVE side chains calculated from the peak area of the OCF$_2$ peak at −81.8 ppm, taking into account the different number of fluorine nuclei.

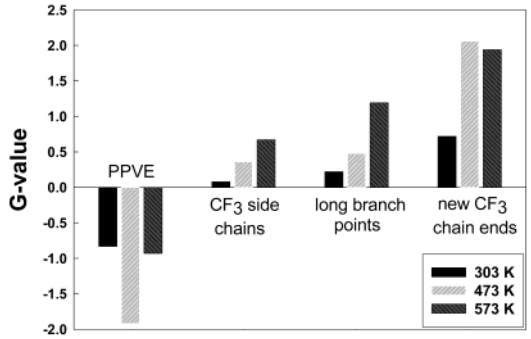

Figure 6. *G* values for PPVE, CF$_3$ side chains, long branch points, and new chain ends for irradiation temperatures of 303, 473, and 573 K.

From the data presented here, it becomes clear that as the irradiation temperature is increased, so too are the number of branch points. While the only new structures in PTFE irradiated at room temperature are CF$_2$CF$_3$ chain ends,[10] in PFA irradiated at 303 K we see small amounts of structures associated with branching as well as chain ends. The T_g of PFA is 363 K as measured by dynamic mechanical analysis (DMA), although it is a broad transition with the onset at approximately 300 K. The small amount of branched structures seen in the sample irradiated at 303 K are presumably due to a slight increase in mobility of the amorphous regions at this temperature. At 473 K the PFA is well above the T_g so that the radicals in the amorphous regions can move freely and form branched structures. At 573 K the PFA is at the onset of the crystalline melting transition, permitting additional chain mobility within the crystallites leading to more branching.

While the NMR spectra show the existence of branching, it is not clear whether a cross-linked network is being formed or simply a highly branched system. The *G* values for new CF$_3$ chain ends are greater than the *G* values for long branch points at each of the temperatures studied. Given the excess of CF$_3$ chain ends over long branch points, in theory each long branch point could be terminated with a CF$_3$ chain end at each

temperature, resulting in a highly branched but not cross-linked system. Between the irradiation temperatures of 473−573 K the *G* values for the long branch points increase while the *G* values for new chain ends remain approximately constant. We might expect that if the irradiation temperature was increased to above the crystalline melting point of 578 K, then the number of long branch points might exceed the number of new chain ends. Fuchs and Scheler showed that PTFE irradiated in the melt exhibited an excess of branch points over chain ends, suggesting that not all branches were terminated with CF_3, but some must react with other chains, forming cross-links.

The system is complicated by the existence of crystalline and amorphous regions and the probable differences in radiation sensitivity between the two phases. It may be that cross-linking predominates over scission in the amorphous regions whereas chain scission dominates over cross-linking in the crystalline regions, the NMR spectra shown here giving an average picture. However, the probability for cage recombination would be expected to be higher in the crystalline regions than the amorphous regions, due to the facile nature of radical−radical reactions and the lower mobility of the fragments of scission reactions in the crystalline phases. One conclusion we can make is that, after irradiation, more short branches are found in the amorphous regions based on the more intense $CF_{3(amorphous)}$ side chain peaks at −71.7 ppm compared with the $CF_{3(crystalline)}$ side chain peak at −68.6 ppm.

Figure 6 shows a large negative *G* value for PPVE units at all temperatures studied. *G* values for loss of side groups in low-density polyethylene with similar branch frequency as for PFA measured using gas chromatography of the volatile products[31] are 2−3 orders of magnitude lower than that observed for the PPVE units here. It could be said that much of the radiation damage in PFA occurs at the comonomer units, possibly due to the larger free volume and lower cage effect at these units compared with the TFE units.

4. Conclusions

High-speed MAS ^{19}F NMR has been used to identify nonvolatile products in semicrystalline PFA following γ-irradiation. When PFA is irradiated at 303 K, the main process is chain scission, while at higher temperatures formation of short and long branches becomes more prominent as does double-bond formation. Perfluoromethyl side chains have been identified in two morphological environments after γ-irradiation. The large negative *G* value for the PPVE comonomer suggests that it is sensitive to radiation.

Acknowledgment. The authors acknowledge the financial support from the Australian Research Council, the Australian Institute of Nuclear Science and Engineering, and the Institute of Polymer Research Dresden (the IPF). Travel by T.R.D. to the IPF would not have been possible without funding from the Francine Kroesen Travel Fellowship. We are especially grateful to Professor K. Lunkwitz for making the facilities available and thank him and Dr. U. Lappan and B. Fuchs for helpful discussions.

References and Notes

(1) Sun, J.; Zhang, Y.; Zhong, X.; Zhu, X. *Radiat. Phys. Chem.* **1994**, *44*, 655−659.
(2) Chapiro, A. In *High Polymers*; Mark, H., Marwell, C. S., Melville, H. W., Eds.; Interscience: New York, 1962; Vol. XV, p 526.
(3) Lappan, U.; Geissler, U.; Lunkwitz, K. *J. Appl. Polym. Sci.* **1999**, *74*, 1571−1576.
(4) Oshima, A.; Seguchi, T.; Tabata, Y. *Radiat. Phys. Chem.* **1999**, *55*, 61−71.
(5) Burger, W.; Lunkwitz, K.; Pompe, G.; Petr, A.; Jehnichen, D. *J. Appl. Polym. Sci.* **1993**, *48*, 1973−1985.
(6) Zhong, X.; Yu, W.; Zhang, Y.; Sun, J. *Polym. Degrad. Stab.* **1993**, *40*, 115−116.
(7) Rosenberg, Y.; Siegmann, A.; Narkis, M.; Shkolnik, S. *J. Appl. Polym. Sci.* **1992**, *45*, 783−795.
(8) Hegazy, E. A.; Dessouki, A. M.; Rabie, A. M.; Ishigaki, I. *J. Polym. Sci., Polym. Chem. Ed.* **1984**, *22*, 3673−3685.
(9) Lunkwitz, K.; Lappan, U.; Lehmann, D. *Radiat. Phys. Chem.* **2000**, *57*, 373−376.
(10) Fuchs, B.; Scheler, U. *Macromolecules* **2000**, *33*, 120−124.
(11) Katoh, E.; Sugishwa, H.; Oshima, A.; Tabata, Y.; Seguchi, T.; Yamazaki, T. *Radiat. Phys. Chem.* **1999**, *54*, 165−171.
(12) Forsythe, J. S.; Hill, D. J. T.; Mohajerani, S.; Whittaker, A. K. *Radiat. Phys. Chem.* **2001**, *60*, 439−444.
(13) Wray, V. In *Annual Reports on NMR Spectroscopy;* Webb, G., Ed.; Academic Press: London, 1980; Vol. 10B, (a) p 28, (b) p 93, (c) p 53, (d) p 54, (e) p 22.
(14) Hintzer, K.; Lohr, G. In *Modern Fluoropolymers: High Performance Polymers for Diverse Applications*; Scheirs, J., Ed.; John Wiley & Sons: New York, 1997; pp 223−237.
(15) Weeks, J. J.; Eby, R. K.; Clark, E. S. *Polymer* **1981**, *22*, 1496−1499.
(16) Starkweather, H. W.; Zoller, P.; Jones, G. A. *J. Polym. Sci., Polym. Phys. Ed.* **1984**, *22*, 1431−1437.
(17) White, M. L.; Waddon, A. J.; Atkins, E. D. T.; Farris, R. J. *J. Polym. Sci., Polym. Phys. Ed.* **1998**, *36*, 2811−2819.
(18) Whittaker, A. K., unpublished results.
(19) Oshima, A.; Tabata, Y.; Kudoh, H.; Seguchi, T. *Radiat. Phys. Chem.* **1995**, *45*, 269−273.
(20) Oshima, A.; Seguchi, T.; Tabata, Y. *Polym. Int.* **1999**, *48*, 996−1003.
(21) Lappan, U.; Geissler, U.; Lunkwitz, K. *Nuc. Inst. Methods Phys. Res. B* **1999**, *151*, 222−226.
(22) Fisher, W. K.; Correlli, J. C. *J. Polym. Sci., Polym. Chem. Ed.* **1981**, *19*, 2465−2493.
(23) Tutiya, M. *Jpn. J. Appl. Phys.* **1972**, *11*, 1542−1546.
(24) Tsuda, M.; Oikawa, S. *J. Polym. Sci., Polym. Chem. Ed.* **1979**, *17*, 3759−3773.
(25) Tabata, Y.; Oshima, A.; Takashika, K.; Seguchi, T. *Radiat. Phys. Chem.* **1996**, *48*, 563−586.
(26) Wray, V. In *Annual Reports on NMR Spectroscopy;* Webb, G., Ed.; Academic Press: London, 1983; Vol. 14, p 22.
(27) Katoh, E.; Sugimoto, H.; Kita, Y.; Ando, I. *J. Mol. Struct.* **1995**, *355*, 21−26.
(28) Dargaville, T. R.; Hill, D. J. T.; Whittaker, A. K. *Radiat. Phys. Chem.* **2001**, *62*, 25−31.
(29) Ciampelli, F.; Venturi, M. T.; Sianesi, D. *Org. Magn. Reson.* **1969**, *1*, 281−293.
(30) Forsythe, J. S.; Hill, D. J. T.; Logothetis, A. L.; Seguchi, T.; Whittaker, A. K. *Macromolecules* **1997**, *30*, 8101−8108.
(31) Bowmer, T. N.; Ho, S.-Y.; O'Donnell, J. H. *Polym. Degrad. Stab.* **1983**, *5*, 449−456.

MA020195Q